



HAL
open science

Structural reliability methods applied to power switch devices: Example of an aeronautical IGBT module

Adrien Zéanh, Olivier Dalverny, Arezki Bouzourene, Christophe Bruzy

► To cite this version:

Adrien Zéanh, Olivier Dalverny, Arezki Bouzourene, Christophe Bruzy. Structural reliability methods applied to power switch devices: Example of an aeronautical IGBT module. *Journal of Mechanical Design*, 2011, 133 (9), pp.1-9. 10.1115/1.4004585 . hal-03472001

HAL Id: hal-03472001

<https://hal.science/hal-03472001>

Submitted on 9 Dec 2021

HAL is a multi-disciplinary open access archive for the deposit and dissemination of scientific research documents, whether they are published or not. The documents may come from teaching and research institutions in France or abroad, or from public or private research centers.

L'archive ouverte pluridisciplinaire **HAL**, est destinée au dépôt et à la diffusion de documents scientifiques de niveau recherche, publiés ou non, émanant des établissements d'enseignement et de recherche français ou étrangers, des laboratoires publics ou privés.



Open Archive TOULOUSE Archive Ouverte (OATAO)

OATAO is an open access repository that collects the work of Toulouse researchers and makes it freely available over the web where possible.

This is an author-deposited version published in : <http://oatao.univ-toulouse.fr/>
Eprints ID : 5954

To cite this version :

Zéanh, Adrien and Dalverny, Olivier and Bouzourene, Arezki and Bruzy, Christophe *Structural reliability methods applied to power switch devices: Example of an aeronautical IGBT module*. (2011) Journal of Mechanical Design, vol. 133 (n° 9). pp. 1-9. ISSN 1050-0472

Any correspondence concerning this service should be sent to the repository administrator: staff-oatao@listes.diff.inp-toulouse.fr

Structural Reliability Methods Applied to Power Switch Devices: Example of an Aeronautical IGBT Module

Adrien Zéanh

Research Engineer

e-mail: adrien.zeanh@enit.fr

Olivier Dalverny

Associate Professor

e-mail: olivier.dalverny@enit.fr

Laboratoire de Génie de Production

Université de Toulouse,

INPT/ENIT,

47, avenue d'Azereix,

Tarbes 65016, France

Arezki Bouzourene

Power Electronics Engineer

e-mail: arezki.bouzourene@fr.thalesgroup.com

Christophe Bruzy

Manager

e-mail: christophe.bruzy@fr.thalesgroup.com

THALES Avionics Electrical Systems

41, boulevard de la république,

Chatou 78401, France

In this paper, an Insulated Gate Bipolar Transistor (IGBT) module designed for aeronautic applications is investigated using structural reliability methods coupled with Finite Elements (FE) modeling. The lifetime of the module with respect to its solder joints failure, is evaluated using its thermomechanical response, in association with a low cycle fatigue model. The simulation of an aeronautic typical Accelerated Thermal Cycling (ATC) test configuration allows checking in a first step, the relevancy of the numerical procedure by assessing the experimental lifetime of the connections, and comparing them to experimental results. Then, the structural reliability of the module is evaluated over the target aircraft predicted useful lifetime, comparing the First Order Reliability Method (FORM) and Monte-Carlo Simulation (M-CS). The appropriate temperature mission profile and flight time are therefore considered with their scatters, in addition to those of the parameters of the fatigue model. Regarding these latter parameters, a simulation based approach is proposed and applied for the determination of their probability density function (pdf). For reasonable reliability analysis time, the thermomechanical response of the module was surrogated using Kriging metamodels. The paper ends with the exploitation of the reliability importance factors for identifying and proposing improvements, with the demonstration of considerable reliability increase.

Keywords: Power Switch Modules, Aeronautic Applications, Finite Elements Modeling, Surrogate Modeling, Lifetime Analysis, Structural Reliability

1 Introduction

One of the current trends in the aircraft industry is the increasing use of electrical systems in replacement of mechanical, hydraulic, and pneumatic ones. This evolution which already led to numerous More Electric Aircraft (MEA) programs, aims at increasing aircrafts performances and reducing onboard equipments weights and volumes as well as their maintenance costs with reliability improvement [1–3]. The ultimate goal of the aeronautic industrial is to increase their leadership and competitiveness, with the reduction of aircrafts operational costs, while improving passengers' security and comfort.

In the proposed and upcoming electrical applications, several power converters are implemented, which each involve several sensitive power switch modules. In addition to their important number, these modules are predicted to be used the most closer to the actuators that they drive. That's to say, they could operate in non pressurized area, under harsh aeronautic stresses. In example, the external temperatures could range from $-63\text{ }^{\circ}\text{C}$ up to $200\text{ }^{\circ}\text{C}$ with ramp reaching $10\text{ }^{\circ}\text{C}/\text{mn}$, in combination with mechanical chocs and vibrations, under pressure and moisture atmosphere [4]. All these circumstances lead the electrical applications to very significant risks of lifetimes and reliability concerns. Among these systems potential failures, those occurring on power modules are the most feared because of their criticality (nondetectability, occurrence, and severity) on the systems electrical function. They were for this reason intensively studied with several publications, in order to investigate their failure modes, and then improve their lifetimes and reliability [5,6].

In this paper, structural reliability methods are implemented to analyze a prototype of power module developed for a harsh aeronautic application (engine zone). These methods particularly suitable for virtual prototyping, are still rarely used for mechanically complex products, and particularly power electronic switch components, probably because of the numerical challenge of this task, with the consideration of generally important number of failure scenarios involved, the complexity of the numerical modeling of the failures scenarios, the computational cost required for accurate numerical results, the availability of relevant models of the scatter of the preponderant design variables, etc.

These questions are examined herein, after a brief recall of the principle of structural reliability calculations and its applicability to power modules. The technology of the considered module is presented, before highlighting the criticality of solder joints thermomechanical fatigue, formulating the relating Limit State Function (LSF) and presenting the Finite Elements (FE) model. In order to minimize the computational cost involved in structural reliability procedures, the response of the FE model is surrogated using Kriging. For the reliability analysis, the temperature mission profile and flight time are considered with their scatters, in addition to those of the parameters of the fatigue model. Regarding these latter parameters, a simulation based approach is proposed and applied for the determination of their probability density function (pdf). Then, the performance of the module is evaluated in two configurations: a test configuration and the real mission profile configuration. The analysis results are discussed and the importance factors exploited to highlight technical solutions which increase the reliability of the module.

2 Reliability Analysis Approach

In the fields of reliability engineering, the common approaches for systems or products reliability analysis consist in aggregating the reliabilities of their individual components, accounting for their interactions within the system function, and their potential failures modes. The usual techniques used are based upon the use of combination of qualitative and quantitative representations and modeling methods, such as Failure Modes, Effects and Criticality Analysis (FMECA), Fault Tree Analysis (FTA), Reliability Block Diagrams (RBD), etc [7,8].

Regarding the components, the reliability methods can be classified in two mains families: The life data analysis based methods and structural reliability based methods.

The life data analysis methods were investigated, during the first footsteps of the reliability engineering in the 1950s [9,10]. They are based on failure rates modeling, from field or test life data, making eventually use of Bayesian concepts in order to account for experts judgments, or information often collected on equivalent components or systems operating in similar conditions [11,12]. They present the advantage of being relatively simple for reliability assessment, but suffer from the availability and the quality of the input data, not forgetting the important costs generally required for collecting them. Many handbooks and standards providing components specific information such as the notorious Military Handbook 217F [13] were proposed and widely adopted in the industry [14,15]. However, these handbooks were all founded on various assumptions which validities are not always verified, such as the notorious hypothesis of constant failure rate [16,17].

Structural reliability emerged in the late 1970s, for evaluating the failure probability of structural integrity of offshore structures, buildings, bridges, and other civil constructions [18,19]. It is a component-centric approach that considerably grew since 1980s with the development of rigorous and accurate calculation methods [20,21]. With the maturity of physic-of-failure based lifetime modeling [22] and the computing capabilities, the structural reliability is experiencing an increasing use in many recent industrial fields. It can be fully integrated within virtual prototyping strategy, and appears to date as most accurate and inexpensive for evaluating products in a development phase, in comparison with life data analysis approach.

2.1 Structural Reliability. Fundamentally, the structural reliability approach allows the calculation of the failure probability of a given component with respect to a precise failure mode, considering the scatter of its driving variables. It necessitates:

- the definition of a stochastic model, depending on a set \mathbf{X} of random design variables and parameters characterizing the failure, which obey a joint density function $f_{\mathbf{X}}(\mathbf{x})$;
- the definition with respect to the considered failure mode, of a limit state function $G(\mathbf{x})$ which splits the safe domain (defined by $\{\mathbf{x} \text{ such that } G(\mathbf{x}) > 0\}$) from the failure domain (defined by $\{\mathbf{x} \text{ such that } G(\mathbf{x}) \leq 0\}$). The boundary defined by $\{\mathbf{x} \text{ such that } G(\mathbf{x}) = 0\}$ is called the limit state surface.

From these definitions, the failure probability is calculated by the relation (1):

$$P_f = \int_{G(\mathbf{x}) \leq 0} f_{\mathbf{X}}(\mathbf{x}) d\mathbf{x} \quad (1)$$

The analytic calculation of the above integral is not always possible, and approximation methods such as First Order Reliability Method and Second Order Reliability Method (FORM, SORM), or sampling methods like Monte-Carlo Simulation (M-CS) are used in practice. For the sake of numerical stability, accuracy, and efficiency of the algorithms, these calculations are performed within a standard space, where the physical variables are transformed into uncorrelated, unit variance and zero mean Gaussian random variables, using iso-probabilistic transformations [23]. Within this space, the reliability is measured through the Hasofer-Lind reliability index denoted β_{HL} , which is defined as the number of standard-deviations from the median response to the LSF [24]. In addition to allow the evaluation of the failure probability of the considered component, the structural reliability approach provides information for its optimization, among which the elasticities of its failure probability P_f or its reliability index β_{HL} to the design variables statistical distribution parameters (2):

$$e_{p_{X_i}^j}(\beta) = \frac{p_{X_i}^j}{\beta_{HL}} \frac{\partial \beta_{HL}}{\partial p_{X_i}^j} \Big|_{\mathbf{x}^*} \quad \text{and} \quad e_{p_{X_i}^j}(P_f) = \frac{p_{X_i}^j}{P_f} \frac{\partial P_f}{\partial p_{X_i}^j} \Big|_{\mathbf{x}^*} \quad (2)$$

where $p_{X_i}^j$ represents the j th parameter of the statistical distribution of the variable X_i , and \mathbf{x}^* the Most Probable Point (MPP), i.e., the point of the LSF having the highest probability of being reach. These outputs can be used to point out reliability improvement solutions, within iterative reliability and optimization nested procedures, such as those used in reliability based design Optimization (RBDO) [25–27].

2.2 Applicability to Systems With Multiple Failure Scenarios.

The practical application of structural reliability methods to complex systems generally remains a challenging task, due to the management of several failure modes, with their possible interactions. It can be addressed according to two basic approaches: the multiple limit states (MLS) approach and the minimal cut sets (MCS) approach.

In the MLS approach, the feared failure scenarios are combined within the definition of a unique LSF [28–30], before running the reliability analysis procedure. This approach appears simple in terms of implementation, but involves numerical difficulties and inaccuracies with traditional approximation methods (FORM/SORM) because of strong nonlinearities and singularities of the resulting LSF. Only the sampling methods are appropriated for such problems [30], with the drawbacks of necessitating excessive computation time for accurate failure probability and sensitivity analysis results.

In the MCS approach, all the minimal cuts, i.e., sequences of individual component failures leading to overall system failure are identified, and the probability of each sequence is evaluated from those of its involved components, considering their interactions and implications in the performance of the system. Then, the structural failure probability of the system is given by the probability of the union of all the sequences.

Compared with the MLS approach, this second approach allows going further in the system reliability analysis, with the exploitation of the reliability analysis results of the different components (failure probability and importance factors). It gives a better insight of the system failure mechanisms with the clarification of components interactions, and offers additional information for prioritizing improvement efforts with the possibility of computing criticalities and reliability importance measures of the components within the system [31–34].

For the particular case of power switch modules, the second approach appears as most appropriated, as these modules are subjected to several preponderant failure scenarios with the particularity that the module fails when only one of the scenarios realizes (see Sec. 3.2 below). Hence, the minimal cuts resume in the set of preponderant failure events. Denoting n_{ev} the number of considered failure events (E_i), the failure probability ($P_f(\text{module})$) of a given module results in the probability of the union of all the E_i :

$$P_f(\text{module}) = P\left(\bigcup_{i=1}^{n_{ev}} E_i\right) \quad (3)$$

3 Presentation of the Power Switch Module

3.1 Description. The power module studied herein was developed within the MODular ElectRical NETwork (ModErNe) MEA research program with THALES Avionics Electrical Systems. It is an elementary switch consisting of 4 chips (2 IGBT and 2 diodes) brazed on a metallized AlN substrate and an Al-SiC base plate, the electrical connections being achieved through a top substrate by power bumps (Fig. 1). It's structure exhibits better electrical and thermal performances of converters, while leading to lower weight, volume, and cost in comparison with the previous packaging technologies, particularly for water cooled three-phase converters [35].

As shown on Fig. 1 and reported in various overviews of power switch components [5], almost all of the modules technologies employ low melting point solders to ensure their mechanical assembling. For this packaging, the assembling process required

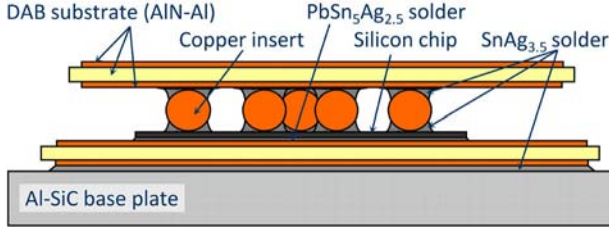


Fig. 1 Structure of the power switch module with aluminium metallizations

the use of two solders with high and low melting points. $\text{Sn}_{96.5}\text{Ag}_{3.5}$ (221 °C of melting point) and $\text{Pb}_{92.5}\text{Sn}_{5}\text{Ag}_{2.5}$ (292 °C of melting point) were retained as depicted on Fig. 1, with the other parts materials. In addition to their mechanical function, these solders are fully involved in the modules internal electrical connections, while playing an essential role in the evacuation of the thermal power dissipated by the chips when operating.

3.2 Solder Joints Failure. Despite of all the technological improvements achieved, power modules failures remain critical in harsh environments applications, such as aeronautic those where high lifetime (more than 100,000 operating hours or 30,000 flying cycles) and high reliability levels are required. In such environments with wide cyclic temperature swing amplitudes, the solders degradations represent one of the most critical failure modes of power modules, as observed experimentally, shown in several publications [36] and illustrated on Figs. 2 and 3.

These damages are due to the thermomechanical fatigue cumulated over the module lifetime, with the cyclic stresses generated in the assemblies by the combination of Coefficients of Thermal Expansion (CTE) mismatch of the soldered parts, and the cyclic variations of the temperature [35–37]. Their occurrence directly affects the modules electrical function by causing chips excessive heat (burn-out) or by simply interrupting the electrical paths.

3.3 Formulation of the Limit State Function. Regarding solders interconnects lifetime, numerous prediction models were proposed in the literature. Among the usable models, the one proposed by Heinrich [38] was chosen for this study because of its relative accuracy, and simplicity of implementation [39]. This model expresses the lifetime of a given solder joint in terms of mean or characteristic number of thermomechanical cycles before failure, by $N_f = K_1(\Delta W_{\text{ave}})^{K_2}$, with K_1 and K_2 two material dependent parameters, and ΔW_{ave} the damage metric defined as the Averaged Viscoplastic Strain Energy Density (VSED) over the solder joint. The calculation of this metric is performed here using the finite elements (FE) analysis results for each connection, by averaging the VSED of the solder joint elements over its volume: $\Delta W_{\text{ave}} = \sum \Delta W_e V_e / \sum V$ with ΔW_e the dissipated VSED by the e th element and V_e the associated volume.

Considering this fatigue model, the LSF is written:

$$G(\mathbf{x}) = K_1(\Delta W_{\text{ave}}(\mathbf{x}))^{K_2} - N_{\text{target}} \quad (4)$$

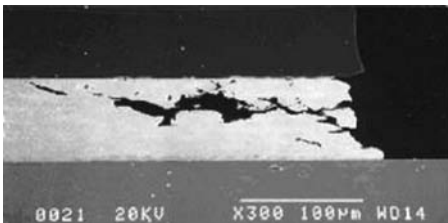


Fig. 2 Die collector solder joint damage after power cycling

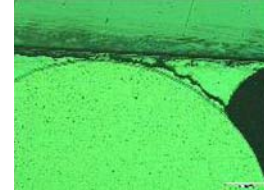


Fig. 3 Bump connection solder joint damage after power cycling

where N_{target} represents the target lifetime in terms of number of cycles that the power module must reach without failure.

4 Finite Elements Modeling

4.1 Geometrical Model. In structural reliability, the accuracy of an analysis is strongly dependant to the quality of numerical model used. In order to consider the module real shapes, sizes, and design, the FE model was built under ABAQUS [40] after importing a computer aided design model of the whole switch module. The Fig. 4 depicts the meshed module, the connections of interest being highlighted.

The connections that will be targeted within the reliability analysis are: the 4 base plate solder corners, the 2 outer mechanical bumps $n^{\circ}1$, the 2 outer mechanical bumps $n^{\circ}2$, the 2 Gate bumps, the 6 outer diode bumps, and the 6 outer IGBT bumps, totaling 22 connections.

4.2 Materials Constitutive Laws. For the different parts of the module, the thermal properties, namely thermal conductivities, specific heats, and densities used in the FE model were gathered from the literature [5,41]. Necessary to describe the transient thermal behavior of the assemblies, they are supposed to be constant for all the materials over the assembling and operating temperature range of the module.

In terms of mechanical constitutive law, a linear thermoelastic law was chosen to model the mechanical behavior of the ceramic substrates, the chips and the base plates, Chaboche's elastoplastic model with combined nonlinear isotropic and kinematic hardening [42] was used for copper and aluminium metallizations in order to better describe their cyclic behavior. The solders, operating at temperatures above the half of their melting points, were described using Anand's unified viscoplastic model [43].

All the elastic constants and hardening parameters were considered temperature dependent. The elastic constants were gathered from Refs. [5,41,44–46]. The metallizations hardening parameters

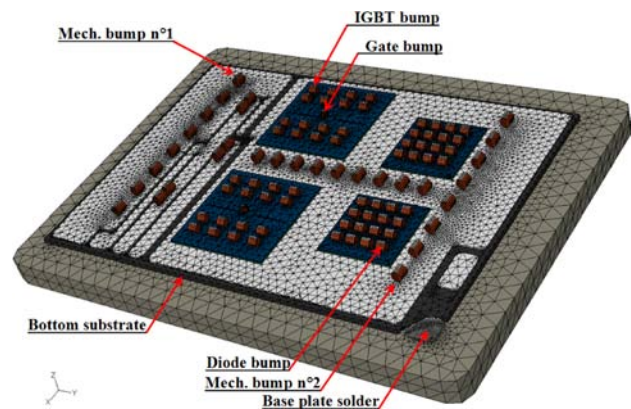


Fig. 4 View of the meshed module, the top substrate being removed and the critical connections highlighted

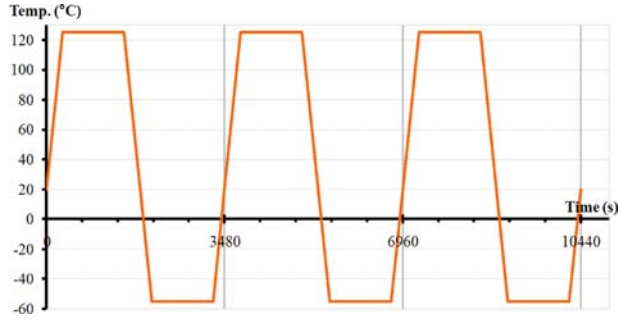


Fig. 5 The ATC temperature profile

were determined by nonlinear optimization results from indentation tests [44]. Anand's parameters were taken from [46] for the $Pb_{92.5}Sn_5Ag_{2.5}$, and identified by running nonlinear optimization on temperature dependant creep and hardening tests results, for the $Sn_{96.5}Ag_{3.5}$ solder [44].

4.3 Boundary Conditions and Loading Profiles. Before simulating the mechanical behavior of the module, the residual stresses induced by the manufacturing step were computed across the whole assembly. The brazing process was therefore simulated from 573 °C to ambient temperature (20 °C) followed by 24 h of storage. Then, two different thermal cycling profiles were considered: an Accelerated Thermal Cycling (ATC) profile used for product qualification and the real loading profile.

The ATC profile was defined according to the method 1010.8 of the Military Handbook 883F [47]. It ranges between -55 and +125 °C, with ramp rates of 20 °C/min and dwell times of 20 min (Fig. 5).

Regarding the real loading profile, it was predicted for this application that the component should operate only a few seconds during the flight cycle. Therefore, the thermal ageing due to chips power dissipation was neglected besides the external thermal loading. For this last one, the International Standard of Atmosphere (ISA), made it possible to determine the module external temperature profile during the plane flight time with its statistical distribution. The Fig. 6 depicts the temperature profile during a flying cycle. For the application considered here, the parking and taking off time are supposed to be deterministic and equal to 2000 s, while the flight time (t_F) is supposed to follow a Gaussian distribution of mean $\mu_{t_F} = 23,400$ s and standard-deviation $\sigma_{t_F} = 3600$ s. The temperature swing amplitude during the flight cycle remains constant and equal to 50 °C, so that the profile is entirely determined by the value of the maximal temperature T_{MAX} . It was also estimated through data collected over a year of flights, that this maximal temperature could be represented by its statistical distribution using a Weibull probability density function. The identification procedure yields $\beta_{T_{MAX}} = 7.87$ as shape

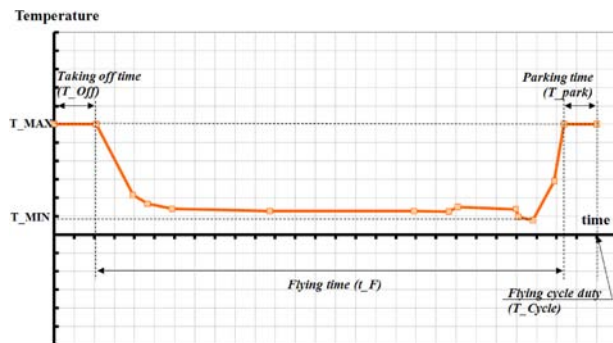


Fig. 6 ISA parameterized temperature loading profile

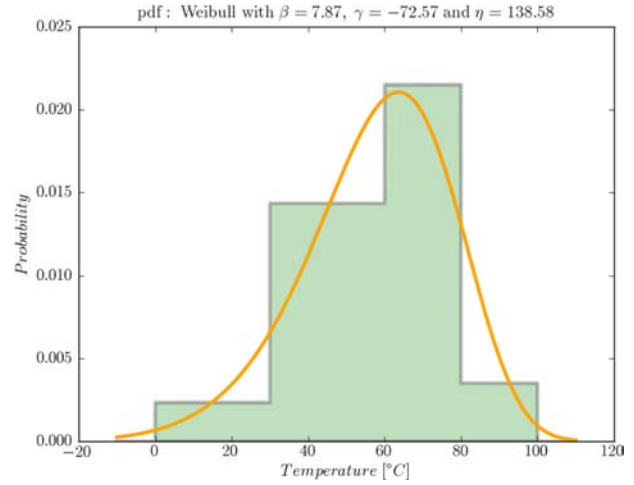


Fig. 7 ISA maximal temperature statistical distribution for an engine zone application

parameter, $\gamma_{T_{MAX}} = -72.57$ °C for the location parameter, and $\eta_{T_{MAX}} = 138.58$ °C for the scale parameter (Fig. 7).

5 Simulation Results and Reliability Assessment

The open source software OpenTURNs [48] is adopted in this study for the reliability calculations.

For the evaluation of connections lifetimes under a given loading profile, the cyclic VSED must be evaluated for the targeted connections, after the stabilized response of the finite element (FE) model was obtained. This state was found to be reached after the first five simulated cycles, with less than 4% of cyclic VSED variation, under all simulated loading profiles. The Figs. 8 and 9 show the VSED distribution in base plate and power bump solder joints, for the most representative loading profile ($T_{MAX} = 60$ °C and $t_F = 27,000$ s).

The VSED distribution in the base plate solder joint is consistent with experimental observations [36,37], showing that the crack in large area solders propagates from solder joint periphery. Then, for more accuracy in predicting the base plate solder joint failure, ΔW_{ave} is evaluated in the joint corner elements (Fig. 8). Regarding bump solders, the corresponding ΔW_{ave} were evaluated in their whole volume because of relatively small size.

In terms of computation time, the simulation (on a 64-bit PC with 8 CPU of 4 GHz and 12 Go of RAM) of a loading profile typically necessitates at least 5 h. Since the reliability methods generally require several hundreds of calls to the numerical model before fulfilling their own convergence criteria, the direct coupling of the FE model with the reliability code can easily lead to

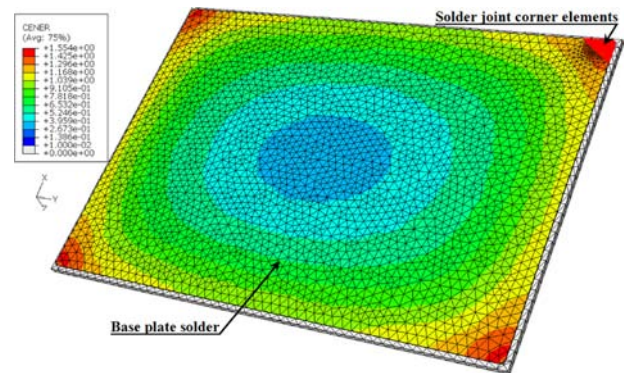


Fig. 8 VSED distribution in base plate solder after five most representative flight cycles $\left[\frac{mJ}{mm^3} \right]$

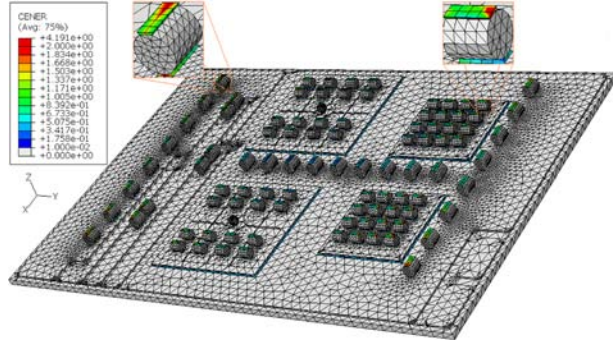


Fig. 9 VSED distribution in bumps solder after five most representative flight cycles $\left[\frac{\text{mJ}}{\text{mm}^3}\right]$

several months for an analysis, which could be redhibitory during product development step. Moreover, the FE simulations often fail to complete due to inappropriate software settings, resulting in numerical problems during the reliability calculation. For all these reasons, the use of a fast executing and continuous surrogate model for approximating the various solder joints cyclic responses is essential.

5.1 Surrogating the Connexions Cyclic VSED Under Real Loading Profile. Traditionally, polynomial Response Surface Models (RSM) were used to surrogate the responses of FE model in structural reliability [49–51], mainly because of the simplicity of their implementation. During the last decade, other types of models such as Artificial Neural Networks (ANN) [52], Krigings [53,54], or Support Vector Machines (SVM) [55] were introduced, with more accurate results in the reliability analyses due to their highest fitting capabilities in comparison with polynomial RSM. In this paper, a Universal Kriging with full quadratic drift was chosen, with a Gaussian semi-variogram model which parameters were fitted on the input data. In order to facilitate the coupling of the surrogate model with OpenTURNS, it was implemented in python scripting language [56]. The reader is invited to refer to [57,58] for more details on the Kriging methods, their applicability and implementation.

The initial data set used for setting the three models parameters was generated using a central composite design of experiments in the domain defined by the two variables defining the loading profile, i.e., the maximal temperature (T_{MAX}) ranging from 0 to 100 °C, and the flight time (t_f) ranging from 16,300 to 30,700 s. This design was filled with selective additional points in order to increase the predicting capabilities of the Kriging metamodels.

In a separate comparison (not presented here), the authors found the Kriging superior to radial basis function neural networks and traditional full quadratic polynomial response surface, regarding their descriptive and predictive capabilities. Moreover, the Kriging provides a predicting variance that can be used to quantify the quality of the initial design plan, and enrich it with smartly chosen points for further accuracy improvement [59].

The results of the kriging approximation is illustrated on the Fig. 10 for the mechanical bump $n^{\circ}2$ solder, with the associated plot of the descriptive and predictive goodness of the data fitting (Fig. 11). The dots on the surface plot indicate the true responses at the sampling points.

5.2 Solders Failure Model Parameters Scatter Modeling. As reported in several publications [60–64], the experimental test times to failure used for identifying the fatigue model parameters present important scatters for a given test configuration. These scatters, mainly linked to the module manufacturing process are generally modeled using a Weibull distribution, in which the scatter of the data is traduced by the shape parameter β_{tff} . The greater the scatter of the data, the lower β_{tff} .

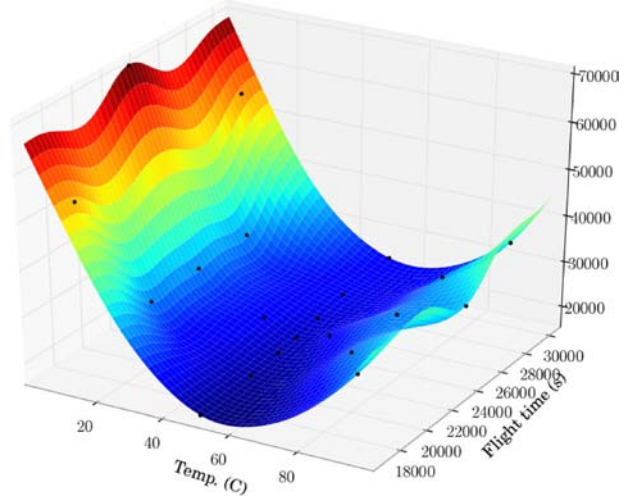


Fig. 10 Kriging plots for the mechanical bump $n^{\circ}2$ solder VSED $\left[\frac{\text{J}}{\text{m}^3}\right]$

To date, too few publications dealt with the impact of these scatters on the reliability of solders joints. Moreover, the available works on this topic only proceed to sensitivity studies which showed the considerable impacts of these scatters on the connections times-to-failure and reliabilities [63]. The consideration of these scatters in the analysis of solders joints structural reliability studies was not investigated, probably because of the unavailability of the statistical distributions of the parameters of their failure models, and the difficulty of their characterization. Without assumption on the parameters distributions models as done in Ref. [63], the determination of analytical expression of the parameters statistical distribution remains challenging. Then, to overcome the complexity of this task, a maximum likelihood estimation coupled simulation procedure is proposed, which is based on the simulation of the failure model parameters reidentification as outlined hereafter:

- (1) consider the solder fatigue model and its two parameters as input data;
- (2) determine the Weibull's shape parameter (β_{tff}) of the connections times-to-failure from test results;
- (3) define a set of $n_{\text{pts}} \geq 2$ values of VSEDs representative of the connections;
- (4) calculate the n_{pts} Weibull's characteristic times-to-failure corresponding to the values of VSED in the previous set, using the input fatigue model;
- (5) calculate n_{pts} Weibull's probability density functions (pdf), with the n_{pts} previous characteristic times-to-failure as scale parameters, β_{tff} as shape parameters and 0 as location parameter;
- (6) simulate a statistically significant number (N_s) of samples of n_{pts} times to failure each, according to the n_{pts} previous Weibull's pdf;
- (7) for each of the N_s samples, reidentify the two parameters, to yield two populations of N_s realizations of the parameters;
- (8) then, identify the statistical distributions of the parameters, comparing different applicable statistical models, i.e., Gaussian, Log-normal, Weibull, Gumbel, etc.

This procedure was applied here for $\text{Sn}_{96.5}\text{Ag}_{3.5}$ solders, with the parameters provided by Zhang et al. [65], $n_{\text{pts}} = 10$ regularly spaced VSED ranging from 0.4 to $1.9 \frac{\text{mJ}}{\text{mm}^3}$, and $N_s = 3000$ samples of times-to failure simulated. Due to a lack of representative test results on the studied power module which is still in a design stage, the worst experimental time to failure Weibull's shape parameter β_{tff} reported in the literature on solder joints was considered, that is to say $\beta_{\text{tff}} = 2.3$ from [64]. This value was observed

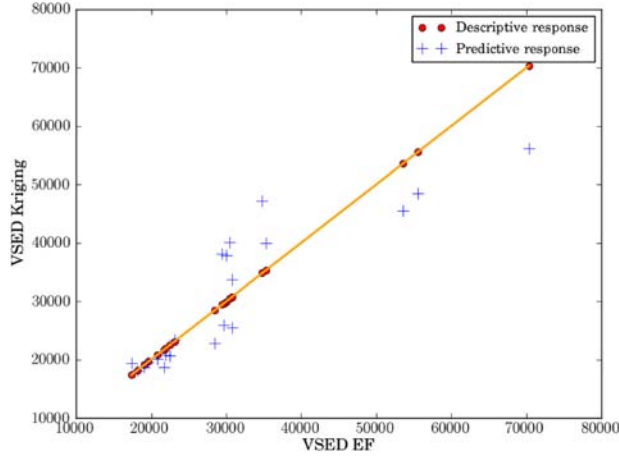


Fig. 11 Goodness of fit of the FE output with the Kriging model on the mechanical bump $n^{\circ}2$ solder joint

on $\text{Sn}_{95.5}\text{Ag}_4\text{Cu}_{0.5}$ solder bumps, among other values ranging from 6 to 8 in Ref. [60], 2.6 and 4.2 for SnPb solder connections in [61], and 2.6 for eutectic SnPb solder connections in [62].

As a result, K_1 was found to follow a Weibull model with $\beta_{K_1} = 0.35$, $\gamma_{K_1} = 0$, and $\eta_{K_1} = 2.38 \times 10^{13}$ as shape, location and scale parameters respectively, and K_2 was found to follow a Gaussian model with $\mu_{K_2} = -1.96$ and $\sigma_{K_2} = 0.356$ as mean and standard deviation respectively. The simulation generated data histograms and the corresponding fitting probability density functions are presented on Figs. 12 and 13 for the two parameters.

5.3 Reliability Analysis

5.3.1 Module Lifetime Analysis Under ATC. In a first step, the ATC times-to-failure of the various connections considered in the module are estimated. This was done considering a Weibull distribution with a shape parameter equals to $\beta_{\text{trf}} = 2.3$, and characteristic lifetime equals to $N_f(63.2\%) = N_f(50\%) \cdot (\Gamma(1 + \frac{1}{\beta_{\text{trf}}}))^{-1}$. The numbers of cycles to failure at various reliability levels are then evaluated by the relation $N_f(P_f) = N_f(63.2\%) \cdot (-\ln(1 - P_f))^{\frac{1}{\beta_{\text{trf}}}}$. The results for the ATC are given in Table 1.

The ranges of estimated numbers of cycles of the different solder joints failure (from 50% to 99% of failure) complies with

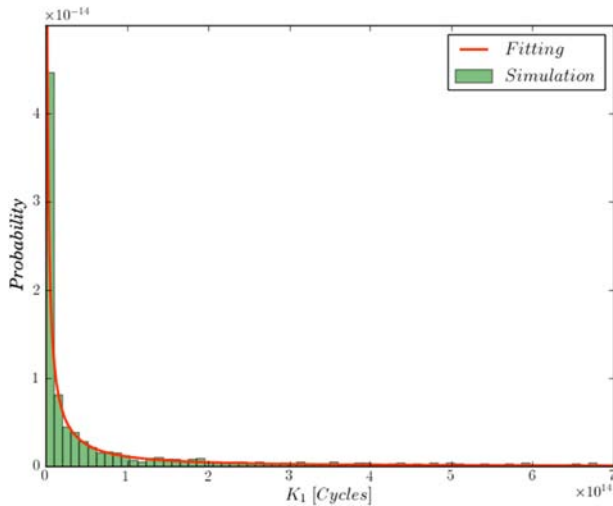


Fig. 12 Plot of the identified pdf of K_1

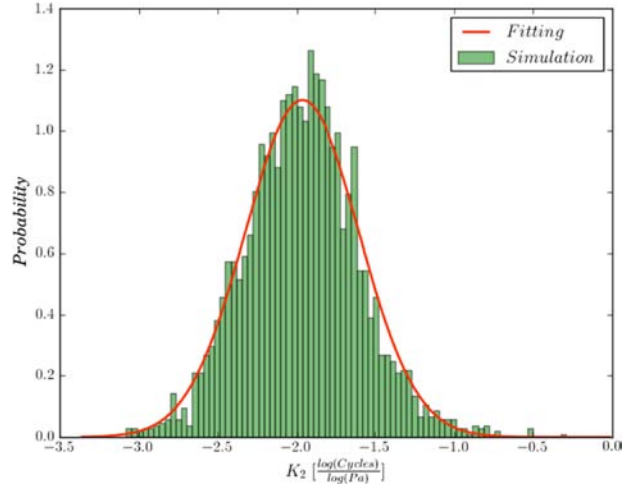


Fig. 13 Plot of the identified pdf of K_2

those generally observed on similar power modules under equivalent thermal cycles tests [35,37]. This is an indicator of the validity of the numerical model, i.e., the finite element model combined with the failure model, to traduce the failure behavior of power modules.

From another stand point, it was estimated basing on the aeronautic standard RTCA/DO-160D and the method 1010.8 of the Military Handbook 883F, that the module should withstand at least 2000 cycles of the considered accelerated thermal loading without failure, in order to qualify for the target application [47,66]. Considering this requirement, the above results point out needs of improvements. These are investigated in the next section, with the evaluation of the reliability of the module under the real loading profile.

5.3.2 Module Reliability Under the Real Loading Profile. The required lifetime without failure for this module in its target application is of 30,000 flight cycles. In order to evaluate its capability of satisfying this requirement, the failure probabilities (P_f) of its most critical connections were computed over the required lifetime. This was done using the surrogate models previously built, under the reliability software OpenURNS. In a first step, the Hasofer-Lind reliability index (β_{HL}) was computed for each connection, followed by the FORM failure probability, and then, the M-CS failure probability. Table 2 presents the results obtained for the critical solder joints.

At first glance, the results in Table 2 allow to hierarch the different connections. They demonstrate, in compliance with the ATC simulation results, that the mechanical bump $n^{\circ}1$ is the weakest connection in the module.

From these results and considerations, the failure probability of the module ($P_f(\text{module})$) is assessed considering all its critical

Table 1 ATC simulation results: stabilized cyclic average VSED in Solders and numbers of cycles to failure for various reliability levels

	VSED	$N_f(50\%)$	$N_f(63.2\%)$	$N_f(90\%)$	$N_f(95\%)$	$N_f(99\%)$
Base plate	418,623	986	1113	1600	1794	2163
Diode bump	652,542	413	466	670	752	906
IGBT bump	640,392	429	484	695	780	940
Gate bump	328,691	1585	1789	2571	2882	3475
Mech. bump 1	687,447	373	421	605	679	818
Mech. bump 2	624,009	451	509	732	820	989

Table 2 Critical solder joints reliability analysis

Connection	β_{HL}	FORM P_f	M-CS P_f
Base plate	0.234	0.41	0.46
Diode bump	-0.038	0.52	0.57
IGBT bump	-0.033	0.51	0.54
Gate bump	0.942	0.17	0.18
Mech. bump 1	-0.143	0.56	0.57
Mech. bump 2	-0.024	0.51	0.54

connections, through the relation 3 which expands using the Poincaré formulae:

$$P\left(\bigcup_{i=1}^{n_{ev}} E_i\right) = \sum_{i=1}^{n_{ev}} P(E_i) - \sum_{j=2}^{n_{ev}} \sum_{i=1}^{j-1} P(E_i \cap E_j) + \dots + (-1)^{n_{ev}} P(E_1 \cap E_2 \cap \dots \cap E_{n_{ev}}) \quad (5)$$

In this expanded expression, the rigorous evaluation of the failure probability of each intersection of the failure events necessitates the calculation of conditional probabilities, as shown for two events in the relation 6.

$$P(E_i \cap E_j) = P(E_i)P(E_j|E_i) \quad (6)$$

with $P(E_j|E_i)$ the probability of E_j knowing that E_i occurred. In brief, in addition to the probabilities of the individual events, the calculation of failure probability of the module through the relation 5 requires conditional events probabilities, which must be evaluated for each other, by running a particular structural reliability analysis of a specific configuration of the module. Because the number of these auxiliary probabilities strongly increases with the number of individual events considered, this becomes redhibitory for such modules due to the important number of connections. The calculation effort of the events intersections probabilities could be drastically avoided under the simplifying hypothesis of events independency, but this assumption does not hold in this case. As an alternative, they are approximated by the probability of the event in the intersection having the lowest probability. This approximation can be legitimated by the fact that, once the weakest connection in the intersection fails, the lifetimes of the other connections will be drastically shortened due to the mechanical weakening of the packaging. In other words, the failure events E_i can be reasonably supposed to be concomitants. Hence, the failure probability of the module is approximated by:

$$P\left(\bigcup_{i=1}^{n_{ev}} E_i\right) \approx \sum_{i=1}^{n_{ev}} P(E_i) - \sum_{j=2}^{n_{ev}} \sum_{i=1}^{j-1} \min\{P(E_i), P(E_j)\} + \dots + (-1)^{n_{ev}} \min\{P(E_1), P(E_2), \dots, P(E_{n_{ev}})\} \quad (7)$$

From this expression, the reliability level of the module is evaluated to 43%, which needs to be increased for satisfying the target application requirements.

5.3.3 Improvement of the Reliability of the Module in Use. It is of interest to note that the previous system reliability calculation assumptions lead the reliability of the module to be closer to that of its weakest connection, namely the mechanical connection $n^\circ 1$. Due to the similitude of the connections inside the module, the improvement actions regarding this connection should positively affect the reliability of the other connections. Hence, the reliability analysis of the module can be linked to that of its mechanical connection $n^\circ 1$. This analysis is performed herein through the analysis of the failure probability elasticities to the parameters of the driving variables statistical distribution. The results obtained are presented on Fig. 14.

From this figure, it clearly appears that the parameters of the fatigue model dominate the environmental variables in the reliabil-

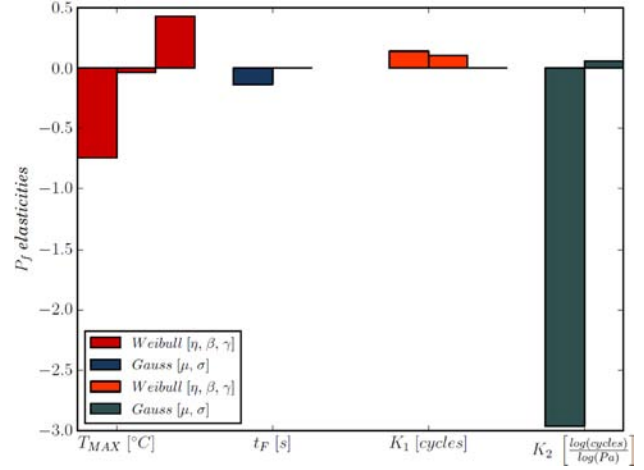


Fig. 14 Mechanical bump $n^\circ 1$ solder joint failure probability elasticities to the variables statistical distributions parameters

ity variation. As solution, the reliability analysis points out some ways of improvement with in this case, the reduction of the scatter on the fatigue models parameters. Efforts must be deployed during the module manufacturing for improving shapes and micro-structure of solder joints repeatability and reproducibility.

Assuming improvements in the manufacturing process, with a higher experimental time to failure Weibull's shape parameter equivalent to these reported by Popelar et al. in Ref. [60], i.e., $\beta_{eff} \approx 7$, a new calculation step yields a reliability level of about 81%, which represents 86% of reliability increase.

Regarding the two other variables, it appears that the statistical parameters of T_{MAX} dominate those of the flight time in the failure probability. Moreover, it is shown that the scatter parameters of these two variables do not have a significant effect on the failure probability, compared to their other parameters. In terms of improvement, the mean flight time fully depends on the use of the target airplane, it is therefore not controllable by the design engineers. Only the temperature can be adjusted by technical solutions like acting on the thermal insulation of the module. For the application considered, these modifications should be leaded such that the Weibull's location and scale parameters of T_{MAX} are respectively decreased and increased, which results in statistically reducing the values of T_{MAX} . Among these two parameters, the location parameter is the easiest to adjust and should be investigated.

Beyond, this qualitative recommendation, the practical engineering question is that of the optimal amount of variation of a given parameter for improving the reliability of a given amount, which does not violate the technical constraints of the application. This question may be solved using the sensitivity analysis results. Under linearity assumption, the amount of variation $\Delta p_{X_i}^j$ for a parameter $p_{X_i}^j$ (the j th parameter of the variable X_i) for increasing the Hasofer-Lind reliability index β_{HL} of $\Delta\beta_{HL}$, can be estimated by the following linear approximation:

$$\Delta p_{X_i}^j = \frac{\Delta\beta_{HL}}{\alpha_{p_{X_i}^j}(\beta_{HL})} \quad (8)$$

where $\alpha_{p_{X_i}^j}(\beta_{HL}) = \left. \frac{\partial\beta_{HL}}{\partial p_{X_i}^j} \right|_{x^*}$ is the sensitivity of β_{HL} to $p_{X_i}^j$ in the neighborhood of the MPP.

Due to the possible high nonlinearity of the LSF, the configuration obtained by this approximation should be validated with a final reliability calculation. In cases of non promising result, an iterative approach should be used. For these calculations, the initial surrogate model can be used if the points involved in the next reliability procedure and the final MPP remain in the domain of validity for which the surrogate model has been built. For the example considered herein, Table 2 showed that, the failure

Table 3 Reliability of the power module for the different improvement scenarios

	Initial configure	$\Delta\gamma_{T_{MAX}} = -6.25^{\circ}\text{C}$	$\beta_{Hf} = 7$	$\beta_{Hf} = 7$ and $\Delta\gamma_{T_{MAX}} = -6.25^{\circ}\text{C}$
β_{HL}	-0.143	-0.106	0.877	0.994
FORM P_f	0.56	0.54	0.19	0.16
FORM reliability (%)	44	46	81	84

probabilities calculated by the FORM and the MCS for the different connections are relatively close (less than 11% of relative error). This traduces the relative linearity of the Limit State Function within the standard normal space. Then, a forward calculation step is expected to yield satisfying results. The sensitivity $\alpha_{\gamma_{T_{MAX}}}(\beta_{HL})$ of the reliability index to the location parameter of T_{MAX} ($\gamma_{T_{MAX}}$) is estimated to -0.008 K^{-1} . Then, the variation of $\gamma_{T_{MAX}}$ for increasing the reliability index of the mechanical bump $n^{\circ}5$ solder joint of 0.05 points, is estimated to $\Delta\gamma_{T_{MAX}} = -6.25^{\circ}\text{C}$. Considering the only decrease of $\gamma_{T_{MAX}}$, the reliability index obtained after running a FORM analysis yields a reliability index of -0.106 , which is relatively close to the one expected and equals to -0.093 . The combination of the experimental times to failure scatter improvement at $\beta_{Hf} = 7$, with a reduction of $\gamma_{T_{MAX}}$ of 6.25°C , in a FORM reliability calculation procedure yields a reliability level of 0.994 (i.e., a failure probability of 0.16 or reliability of 84%). Assuming again that the reliability of the module is linked to the one of the mechanical connection $n^{\circ}1$, its values for the different improvement approach considered are summarized in Table 3.

In addition to these recommendations, technological changes at the power switch module level could also be investigated for further improvements. As an example, it was shown in previous studies [5] that increasing the bumps cylinder sizes or using aluminium instead of copper cylinders could help increasing the corresponding bump solder lifetimes and then reliabilities.

6 Conclusion

A practical application of structural reliability methods to the analysis of power modules was presented, with the particular case of an aeronautic engine zone dedicated device. As observed along the paper, the problem of power modules structural reliability is not only a question of pure reliability methods, but also these of the accuracy of the product F.E. model and the failure model. These points were exposed, with their involved parameters and tried to be answered with the introduction of a Kriging surrogate model of the module. The reliability of the module was analyzed using FORM and Monte-Carlo simulations, which allowed computing and discussing the failure probability of the critical solder joints. Regarding the input variables, the probability density functions of the parameters of the solder joints fatigue model were identified for being taken into account in the analysis. A simulation based identification procedure was therefore proposed and used. These scatter functions were associated with those of the external cyclic temperature profiles of the modules, in order to estimate its performances under ATC test and operating configurations. The analyzes of the reliability importance factors finally helped proposing improvements that considerably increase the reliability of the module. The global procedure was presented, with the corresponding parameters, such that it can be easily applied to equivalent products, in similar operating conditions.

References

[1] Jones, R. I., 1999, "The more electric aircraft: the past and the future?," In IEEE Colloquium on Electrical Machines and Systems for the More Electric Aircraft, Cranfield University, pp. 1-4.
 [2] Quigley, R. E. J., 1993, "More Electric Aircraft," *Proceedings of the IEEE Applied Power Electronics Conference*, San Diego (CA), APEC, pp. 906-911.

[3] Weimer, J. A., 2003, "The Role of Electric Machines and Drives in the More Electric Aircraft," *Proceedings of the IEEE International Electric Machines and Drives Conference*, Vol. 1, pp. 11-15.
 [4] Lhommeau, T., Meuret, R., and Karama, M., 2005, "Technological study of an IGBT module for an aeronautical application in zone engine," In 11th European Conference on Power Electronics and Applications (EPE 2005, Dresden).
 [5] Zéanh, A., Dalverny, O., Karama, M., Woïrgard, E., Azzopardi, S., Bouzourne, A., Casutt, J., and Mermet-Guyennet, M., 2008, "Reliability of the Connections Used in IGBT Modules, in Aeronautical Environment," *Int. J. Simul. Multidiscip. Des. Optim.*, 2(2), pp. 123-133.
 [6] Ciappa, M., 2002, "Selected Failure Mechanisms of Modern Power Modules," *Microelectron. Reliab.*, 42(4-5), pp. 653-667.
 [7] Tang, J., 2001, "Mechanical System Reliability Analysis Using a Combination of Graph Theory and Boolean Function," *Reliab. Eng. Syst. Saf.*, 72, pp. 21-30.
 [8] Sun, Y., Ma, L., Mathew, J., and Zhang, S., 2006, "An Analytical Model for Interactive Failures," *Reliab. Eng. Syst. Saf.*, 91(5), pp. 495-504.
 [9] Saleh, J. H., and Marais, K., 2006, "Highlights From the Early (and Pre-) History of Reliability Engineering," *Reliab. Eng. Syst. Saf.*, 91(2), pp. 249-256. Selected Papers Presented at QUALITA 2003.
 [10] Zio, E., 2009, "Reliability Engineering: Old Problems and New challenges," *Reliab. Eng. Syst. Saf.*, 94(2), pp. 125-141.
 [11] Procaccia, H., and Piepszownik, L., 1992, *Fiabilité des équipements et théorie de la décision statistique fréquentielle et bayésienne*, Eyrolles, EDF, Paris.
 [12] Procaccia, H., and Suhner, M.-C., 2003, *Démarche bayésienne et applications à la sûreté de fonctionnement*, Hermes - Lavoisier, Paris.
 [13] United States Department of the Army, 1991, MIL-HDBK-217F: Military Handbook, Reliability prediction of electronic equipment, Dec.
 [14] Fragola, J. R., 1996, "Reliability and Risk Analysis Data Base Development: An Historical Perspective," *Reliab. Eng. Syst. Saf.*, 51(2), pp. 125-136.
 [15] Bedford, T., and Cooke, R., 2002, "Reliability Databases in Perspective," *IEEE Trans. Reliab.*, 51(3), pp. 294-310.
 [16] Lewis, E. E., 1987, *Introduction to Reliability Engineering*, John Wiley & Sons, New York.
 [17] White, M., and Bernstein, J. B., 2008, *Microelectronics reliability: Physics-of-failure based modeling and lifetime evaluation*, Tech. rep., NASA, Feb. JPL Publication 08-5.
 [18] Madsen, H., Krenk, S., and Lind, N., 1986, *Method of Structural Safety*, Prentice-Hall, Englewood Cliffs, NJ.
 [19] Ditlevsen, O., and Madsen, H., 1996, *Structural Reliability Methods*, Wiley, New York.
 [20] Rackwitz, R., 2001, "Reliability Analysis—A Review and Some Perspectives," *Struct. Saf.*, 23(4), pp. 365-395.
 [21] Lemaire, M., 2005, *Fiabilité des structures: couplage mécano-fiabiliste statique*, Hermès-Lavoisier, Paris.
 [22] Hall, P., and Strutt, J., 2003, "Probabilistic Physics-of-Failure Models for Component Reliabilities Using Monte Carlo Simulation and Weibull analysis: A Parametric Study," *Reliab. Eng. Syst. Saf.*, 80, pp. 233-242.
 [23] Liu, P.-L., and Der Kiureghian, A., 1986, "Multivariate Distribution Models With Prescribed Marginals and Covariances," *Probab. Eng. Mech.*, 1(2), pp. 105-112.
 [24] Hasofer, A., and Lind, N., 1974, "Exact and Invariant Second Moment Code Format," *J. Engrg. Mech. Div.*, 100, pp. 111-121.
 [25] Kharmanda, G., Mohamed, A., and Lemaire, M., 2002, "Efficient Reliability-Based Design Optimization Using a Hybrid Space With Application to Finite Element Analysis," *Struct. Multidiscip. Optim.*, 24, pp. 233-245.
 [26] Youn, B. D., Choi, K. K., and Park, Y. H., 2003, "Hybrid Analysis Method for Reliability-Based Design Optimization," *ASME J. Mech. Des.*, 125, pp. 221-232.
 [27] Adams, B. M., Eldred, M. S., and Wittwer, J. W., 2006, "Reliability-Based Design Optimization for Shape Design of Compliant Micro-Electro-Mechanical Systems," In 11th AIAA/ISSMO Multidisciplinary Analysis and Optimization Conference.
 [28] Zhao, Y.-G., and Ono, T., 1998, "System Reliability Evaluation of Ductile Frame Structures," *J. Struct. Eng.*, 124(6), pp. 678-685.
 [29] Melchers, R. E., and Ahammed, M., 2001, "Estimation of Failure Probabilities of Intersections of Non-Linear Limit States," *Struct. Saf.*, 23(2), pp. 123-135.
 [30] Neves, R. A., Mohamed-Chateauf, A., and Venturini, W. S., 2008, "Component and System Reliability Analysis of Nonlinear Reinforced Concrete Grids With Multiple Failure Modes," *Struct. Saf.*, 30, pp. 183-199.
 [31] Birnbaum, Z. W., 1969, "Multivariate Analysis-II," *On the Importance of different Components in a Multicomponent System*, Academic, New York, pp. 581-592.
 [32] Pan, Z.-J., and Tai, Y.-C., 1988, "Variance importance of system components by monte carlo," *IEEE Trans. Reliab.*, 37, pp. 421-423.
 [33] Meng, F. C., 1996, "Comparing the Importance of System Components by Some Structural Characteristics," *IEEE Trans. Reliab.*, 45(1), pp. 59-65.

- [34] Wang, W., Loman, J., and Vassiliou, P., 2004, "Reliability Importance of Components in a Complex System," Reliability and Maintainability, 2004 Annual Symposium - RAMS, pp. 6–11.
- [35] Mermet-Guyennet, M., 2006, "New Structure of Power Integrated Module," Proceedings of the CIPS.
- [36] Dupont, L., 2006, "Contribution à l'étude de la durée de vie des assemblages de puissance dans des environnements haute température et avec des cycles thermiques de grande amplitude," Ph.D thesis, ENS Cachan, France.
- [37] Micol, A., Zéanh, A., Lhommeau, T., Azzopardi, S., Woïgard, E., Dalverny, O., and Karama, M., 2009, "An Investigation Into the Reliability of Power Modules Considering Baseplate Solders Thermal Fatigue in Aeronautical Applications," *Microelectron. Reliab.*, **49**(9–11), pp. 1370–1374. Proceedings of the 20th European Symposium on the Reliability of Electron Devices, Failure Physics and Analysis (ESREF), October 2009, 5th–9th, Arcachon - France.
- [38] Heinrich, S. M., 1994, *The Mechanics of Solder Alloy - Interconnects*. Van Nostrand Reinhold, New York, ch. 5: Prediction of Solder Joint Geometry, pp. 158–198.
- [39] Bevan, M., and Wuttig, M., 1997, "Complex Fatigue of Soldered Joints - Comparison of Fatigue Models," Electronic Components and Technology Conference, pp. 127–133.
- [40] Dassault Systèmes Simulia Corp., 2009, *ABAQUS Documentation, Version 6.9*. Providence, Rhode Island.
- [41] Ashby, M. F., 2005, *Materials Selection in Mechanical Design*, Butterworth-Heinemann, Oxford.
- [42] Lemaître, J., and Chaboche, J.-L., 1985, *Mécanique des Matériaux Solides*, Dunod, Paris.
- [43] Wang, G. Z., Cheng, Z. N., Beker, K., and Wilde, J., 2001, "Applying Anand Model to Represent the Viscoplastic Deformation Behavior of Solder Alloys," *J. Electron. Packag.*, **123**, pp. 247–253.
- [44] Zéanh, A., 2009, "Contribution à l'amélioration de la fiabilité des modules IGBT utilisés en environnement aéronautique," Ph.D thesis, Université de Toulouse.
- [45] ITRI, 1999, Mechanical properties of solders and solder joints. Tech. rep., International Tin Research Institute. Publication No. 656.
- [46] Wilde, J., Becker, K., Thoben, M., Blum, W., Jupitz, T., Wang, G., and Cheng, Z. N., 2000, "Rate Dependent constitutive relations based on Anand model for 92.5Pb5Sn2.5Ag Solder," *IEEE Trans. Adv. Packag.*, **23**, pp. 408–414.
- [47] United States Department of the Army, 2004. MIL-STD-883F: Test Method Standard Microcircuits, June.
- [48] PhiMeca, EADS & EDF, 2010, *OpenTURNS version 0.13.2 - Reference Guide*.
- [49] Faravelli, L., 1989, "Response-Surface Approach for Reliability Analysis," *J. Eng. Mech.*, **115**(12), pp. 2763–2781.
- [50] Bucher, C. G., and Bourgund, U., 1990, "A Fast and Efficient Response Surface Approach for Structural Reliability Problems," *Struct. Saf.*, **7**(1), pp. 57–66.
- [51] Rajashekhar, M. R., and Ellingwood, B. R., 1993, "A New Look at the Response Surface Approach for Reliability Analysis," *Struct. Saf.*, **12**(3), pp. 205–220.
- [52] Hurtado, J. E., and Alvarez, D. A., 2001, "Neural Network-Based Reliability Analysis: A Comparative Study," *Comput. Methods Appl. Mech. Eng.*, **191**, pp. 113–132.
- [53] Kaymaz, I., 2005, "Application of Kriging Method to Structural Reliability Problems," *Struct. Saf.*, **27**(2), pp. 133–151.
- [54] Kleijnen, J. P., 2007, "Kriging Metamodeling in Simulation: A Review," *Eur. J. Oper. Res.*, **192**, pp. 707–716.
- [55] Li, H.-S., L, Z.-Z., and Yue, Z.-F., 2006, "Support Vector Machine for Structural Reliability Analysis," *Appl. Math. Mech.*, **27**(10), pp. 1295–1303.
- [56] van Rossum, G., 2003, *The Python Language Reference Manual*, Fred L. Drake, Jr., ed., The Network Theory Ltd., United Kingdom.
- [57] Cressie, N. A. C., 1993, *Statistics for Spatial Data*, Wiley, New York.
- [58] Baillargeon, S., 2005, "Le krigeage: revue de la théorie et application à l'interpolation spatiale de données de précipitations," Master's thesis, Faculté des sciences et de génie de l'université Laval, Québec.
- [59] Echard, B., Gayton, N., and Lemaire, M., 2010, "Kriging based Monte Carlo simulation to compute the probability of failure efficiently: AK-MCS method". In 6ème Journées Fiabilité des Matériaux et des Structures et des Structures (JFMS' 10).
- [60] Popelar, S. F., 1998, "A Parametric Study of Flip Chip Reliability Based on Solder Fatigue Modelling: Part II - Flip Chip on Organic," *31st International Symposium on Microelectronics*, pp. 497–504.
- [61] Towashiraporn, P., Subbarayan, G., McIlvanie, B., Hunter, B., Love, D., and Sullivan, R., 2001, "Predictive Reliability Models Through Validated Correlation Between Power Cycling and Thermal Cycling Accelerated Life Tests," Conference on Advances in Packaging (APACK). ISBN No: 981-04-4638-1.
- [62] Darveaux, R., 2002, "Effect of Simulation Methodology on Solder Joint Crack Growth Correlation and Fatigue Life Prediction," *J. Electron. Packag.*, **124**, pp. 147–154.
- [63] Wu, W.-F., Lin, Y.-Y., and Young, H.-T., 2005, "Quantitative Reliability Analysis of Electronic Packages in Consideration of Variability of Model Parameters," *Proceedings of the 7th Electronic packaging technology conference EPTC*, Vol. 2.
- [64] Guédon-Gracia, A., 2006, "Contribution à la conception thermo-mécanique optimisée d'assemblages sans plomb," Ph. D. thesis, Université Bordeaux 1 - France.
- [65] Zhang, Q., Dasgupta, A., and Haswell, P., 2005, "Isothermal Mechanical Durability of Three Selected Pb-Free Solders - Sn3.9Ag0.6Cu, Sn3.5Ag, and Sn0.7Cu," *J. Electron. Packag.*, **127**, pp. 512–522.
- [66] RTCA, 1997. DO-160D: Environmental condition and test procedures for airborne equipment.